Advanced resist testing using the SEMATECH Berkeley extreme ultraviolet microfield exposure tool

Patrick P. Naulleau[a)]
Center for X-Ray Optics, Lawrence Berkeley National Laboratory, Berkeley, California 94720

Christopher N. Anderson
University of California, Berkeley, California 94720

Kim Dean
SEMATECH, Austin, Texas 78741

Paul Denham, Kenneth A. Goldberg, Brian Hoef, and Dimitra Niakoula
Center for X-Ray Optics, Lawrence Berkeley National Laboratory, Berkeley, California 94720

Bruno La Fontaine and Tom Wallow
Advanced Micro Devices, Sunnyvale, California 94088

(Received 10 June 2007; accepted 13 August 2007; published 7 December 2007)

Recent upgrades made to the SEMATECH Berkeley microfield exposure tool are summarized and some of the latest resist characterization results are presented. Tool illumination uniformity covering the full $200 \times 600\ \mu\text{m}^2$ wafer-side field of view is demonstrated and intrawafer focus control of 1.8 nm is shown. Printing results demonstrate chemically amplified resist resolution of 28 nm dense and 22.7 nm semi-isolated. Moreover, contact printing results show that shot noise is not a dominant issue in current 35 nm contact printing performance. © *2007 American Vacuum Society.*
[DOI: 10.1116/1.2781522]

I. INTRODUCTION

With the commercial entry point for extreme ultraviolet (EUV) lithography being pushed towards smaller critical dimensions (CDs), resist issues have become an increasingly important component of the overall EUV technology development task. In the past two years, the ability to simultaneously achieve the required resolution, sensitivity, and line-edge roughness (LER) was determined to be the one of the highest risk problems facing the commercialization of EUV lithography.[1,2] Although the issue of resist resolution and LER is arguably not EUV specific, present source power limitations at EUV wavelengths place stringent constraints on feasible resist sensitivity specifications.

Microfield exposure tools[3–5] play a particularly important role in the area of resist development. This is due to the fact that the relative simplicity of such tools, in general, enables them to provide higher resolution capabilities than full production scale alpha tools.[6,7] Although higher resolution is also available from interference tools, microfield tools have the benefit of more commercially relevant imaging characteristics, in particular, longitudinal characteristics of the aerial image. One such microfield exposure tool dedicated to EUV research is the Berkeley microexposure tool (MET) tool[3,8,9] operating as a SEMATECH resist test center since early 2004. The Berkeley exposure tool utilizes SEMATECH's five times reduction, 0.3 numerical aperture MET optic.[10,11] The MET optic has a well-corrected field of view of $200 \times 600\ \mu\text{m}^2$ at the wafer plane. One of the primary benefits of the Berkeley exposure tool is the fact that it is installed on a highly coherent undulator beamline allowing active illumination components to be used to controllably modify the coherence (pupil fill) in a lossless manner.[12] Such capabilities, in principle, allow the tool to achieve k_1 factors as small as 0.25.

Here, we summarize recent upgrades made to the tool and present some of the latest resist characterization results. The tool illumination uniformity has been improved allowing the full $200 \times 600\ \mu\text{m}^2$ wafer-side field of view to be used. Intrawafer focus control has been improved to 1.8 nm. Resist resolution of 28 nm dense and 22.7 nm semi-isolated has been demonstrated. Moreover, contact printing results have shown that shot noise is not a dominant issue in recent 35 nm contact printing performance.

II. UPGRADES

Two major upgrades have just been completed on the tool: illumination system and focus control. Although beneficial from the perspective of coherence control, the small phase space provided by the undulator illumination has the drawback that beam and/or mirror imperfections are highly persistent upon propagation, making illumination uniformity hard to achieve. To address this issue, the illuminator has been expanded to incorporate homogenizing fly-eye components enabling consistent, robust, and uniform illumination over the entire $1 \times 3\ \text{mm}^2$ object-side field of the MET.

A pair of diamond-turned cylindrical lenslet arrays (fly-eye mirrors) is used to map small neighboring sections of the incoming illumination footprint to the same physical location (the surfaces of the Fourier-synthesis scanning mirrors), wherein the region of overlap is highly uniform in intensity. To further enable control over the illuminated field size, the

[a)]Electronic mail: pnaulleau@lbl.gov

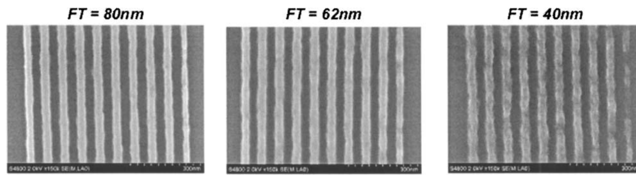

FIG. 1. Example of image degradation in resist as the film thickness is reduced presumably due the interface effects. 40 nm lines and spaces printed in a chemically amplified resist using monopole illumination in the Berkeley MET are shown. As labeled FT, film thicknesses are nominally 80, 60, and 40 nm and the corresponding LERs are 3.7, 4.2, and 7.1 nm, respectively.

overlap region is designed to fill a 1×1 mm^2 subset of the field and the fly-eye mirrors are mounted to scanners similar to those used for coherence control. To eliminate potential interference effects between overlapping beams emerging from different lenslets, we offset each cylindrical element in the fly-eye mirrors by a distance greater than the approximately 500 nm illumination coherence length. A detailed description of this system as well as characterization results can be found in Ref. 13.

The second major upgrade performed on the system was to the focus control mechanism. Focus actuation of the wafer stage is provided by a piezodriven stage and wafer-height sensing is provided by a glancing-incidence laser probe.[14] Due to wafer-height sensor speed limitations before the upgrade, real time piezoactuation feedback was provided by integrated strain gauges. In this configuration, the wafer-height sensor would be used to take one measurement, and the piezosystem would then be told how far to move in order to bring the system to the target height (focus) value. The upgrade involved significantly increasing the speed of the wafer-height sensor, thereby allowing it to be directly used as the piezoactuation feedback bypassing the strain gauges. The benefit of this new configuration has been twofold: improved wafer-to-wafer focus control as well as improved intrawafer focus control. Prior to the upgrade, the wafer-to-wafer rms focus stability was approximately 90 nm, which improved to approximately 49 nm after the upgrade. More importantly, the intrawafer focus control was improved from 21.4 nm before the upgrade to 1.8 nm after the upgrade.

III. RESIST CHARACTERIZATION RESULTS

As target resolutions are pushed smaller, film thickness reductions are required to avoid pattern collapse problems caused by large aspect ratios. One might also expect imaging performance to improve in these thin films simply based on the expected improvement in aerial image quality throughout the volume of the stack. However, as films push below the 100 nm thickness level, interface effects start to become more important. Figure 1 shows an example of image degradation in resist as the film thickness is reduced presumably due the interface effects. The 40 nm lines and spaces printed in a chemically amplified resist using monopole illumination in the Berkeley MET are shown. The film thicknesses are nominally 80, 60, and 40 nm and the corresponding LERs are 3.7, 4.2, and 7.1 nm, respectively. The sensitivity (exposure to size) in all three cases was approximately 11 mJ/cm^2; thus, resist thickness was found to have no measurable impact on resist sensitivity. Based on the LER performance, we find the process to be stable down to 60 nm and then degrade quickly. Assuming that the degradation is due to interface effects, it may be possible to mitigate through the use of bottom antireflection and/or top coats. Note that, in this case, the additional coats would not serve their conventional purpose but would rather simply be introduced for interface control properties.

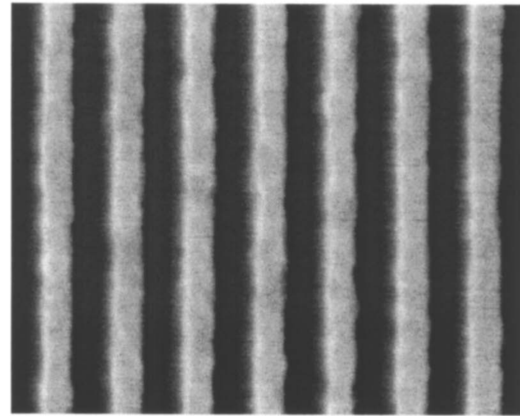

(a)

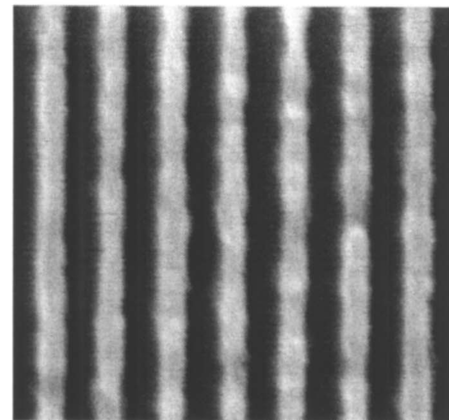

(b)

FIG. 2. Semi-isolated feature printing through exposure control of equal-line-space coded mask features. (a) 27 nm lines on a 70 nm pitch with 3.0 nm LER, and (b) 21 nm lines on a 60 nm pitch with 4.0 nm LER.

As shown elsewhere,[15] resist resolution at the 28 nm dense level is now relatively a routine in the SEMATECH Berkeley MET tool. Even finer resolution has been achieved for semi-isolated features. Figures 2 and 3 show a series of such images achieved in a commercial supplier chemically amplified resist with a sensitivity of approximately 19 mJ/cm^2 (exposure to size) provided by SEMATECH. In Fig. 2, the features are coded as equal lines and spaces on the mask and exposure control is used to reduce the feature size at a fixed pitch. Figure 2(a) shows 27 nm lines on a 70 nm pitch with 3.0 nm LER, and Fig. 2(b) shows 21 nm lines on a 60 nm pitch with 4.0 nm LER. Further shrinking is not possible due to the onset of top loss. Figure 3, on the other

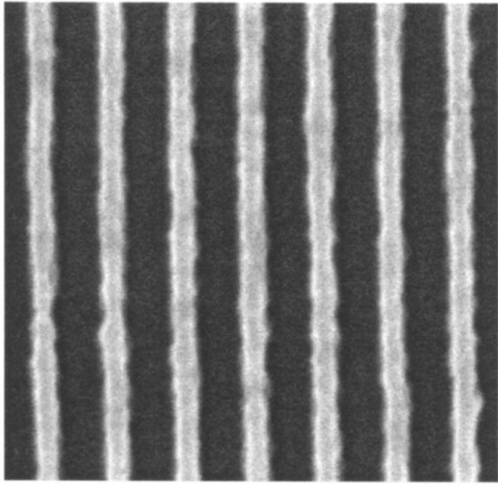

FIG. 3. Semi-isolated lines of 22.7 nm with an LER of 4.0 nm. Features coded as 22.5 nm lines on a 67.5 nm pitch on the mask. The top loss also appears to be less severe than in the overexposed case in Fig. 2(b).

hand, shows features coded as 22.5 nm lines on a 67.5 nm pitch. The actual printed size is 22.7 nm with an LER of 4.0 nm. The top loss also appears to be less severe than in the overexposed case in Fig. 2(b). The illumination setting used for both Figs. 2 and 3 was *y* monopole.

IV. CONTACT-HOLE PRINTING RESULTS

Owing to the larger k_1 factor and, consequently, low mask error enhancement factor (MEEF) the EUV lithography affords, EUV provides significant benefits over immersion 193 nm lithography in printing contacts. Figure 4 shows a series of contacts of various CDs printed in a 80 nm thick layer of chemically amplified Rohm and Haas resist using a conventional binary mask and conventional annular illumination in the Berkeley MET tool. Dose to clear for this resist is approximately 10 $\mathrm{mJ/cm^2}$. For smaller contact sizes, a significant size variation across the small field is evident by eye. As demonstrated in Fig. 5, however, this variation is not a result of shot noise as one might reflexively assume. Figure 5 shows the same 35 nm contacts from Fig. 4 at two different dose and focus settings. Notice that, in each exposure, the relative size relationships between the individual contacts remain fixed. Were the variation a result of shot noise (either from random arrival of photons or any other random event in the resist), the size variation would certainly be uncorrelated from exposure to exposure.

Not being a result of random exposure effects, we conclude that the variations are attributable to the mask. Thus, we use modeling to predict the MEEF for the MET optic when printing 35 nm 1:2 contacts. Figure 6(a) shows the simple binary input mask used in the modeling. One contact in the field is made 2.8 nm smaller $(1\times)$ than the remainder of the 35 nm contacts in the field. Figure 6(b) shows the resulting resist image assuming an ideal binary resist. From this result, we find the MEEF to be only 1.2 and likely not

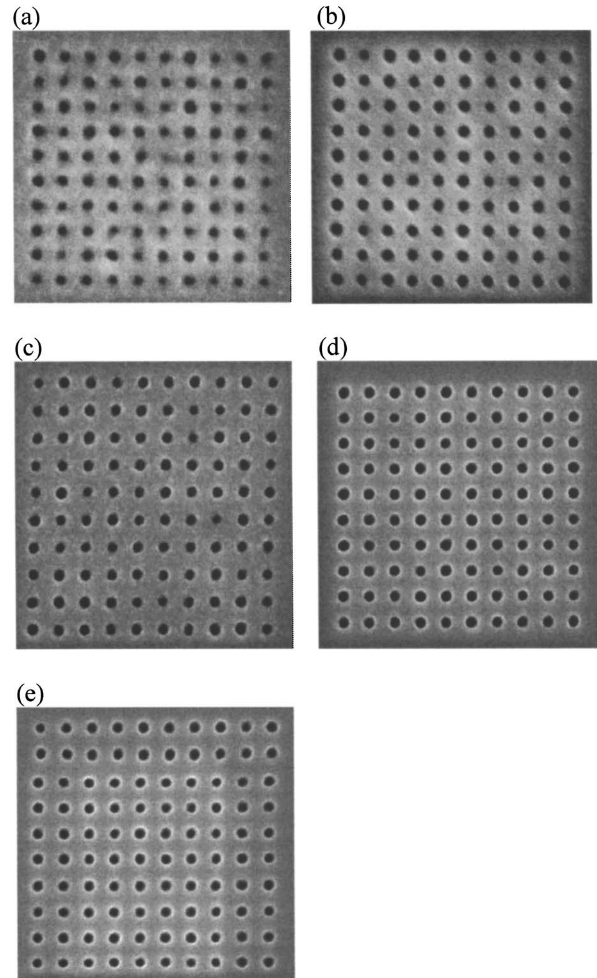

FIG. 4. Contact holes printed in a 80 nm thick layer of Rohm and Haas resist using the Berkeley MET tool with a conventional binary mask and conventional annular illumination $(0.35<\sigma<0.55)$.

large enough to explain the variations seen in Fig. 5. We note that the modeling includes the full wave front information for the MET optic.[16–18]

Next, we consider a more realistic resist model using the point-spread function resist modeling approach.[19–21] Based on independent characterization of the resist used here, we set the resist blur value to 20 nm. The resulting resist image is shown in Fig. 6(c), yielding a MEEF of 3.75. Considering the 1.1 nm rms contact-size variation (wafer coordinates) observed on a similar field on the mask (35 nm 1:1 contacts), we find the predicted resist contact-size variation to be 4.1 nm rms, which is quite close to the 3.2 nm variation observed experimentally.

V. SUMMARY

The SEMATECH Berkeley MET tool has recently been upgraded to support 10% illumination uniformity across the entire $200\times600\ \mu\mathrm{m}^2$ wafer-side field of view. Also, intrawafer focus control has been improved to 1.8 nm. The Berkeley tool continues to drive development and has been used to demonstrate resist resolution of 28 nm dense and 22.7 nm

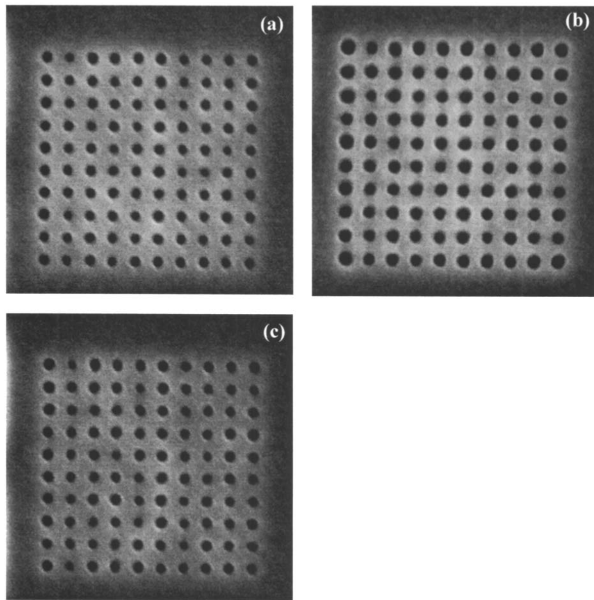

FIG. 5. Three different exposures of 35 nm 1:2 contact holes on one wafer. (b) is at best dose and focus, (a) is best focus and 15% underdosed, and (c) is 15% underdosed and 50 nm defocus.

semi-isolated. Moreover, we have demonstrated that the significant size variation observed in 35 nm contact-hole printing is not a result of shot noise. Rather, the effect is attributable to the MEEF induced by the resolution limit of the resist. Note that the MEEF of the optical system itself is negligible at this feature size.

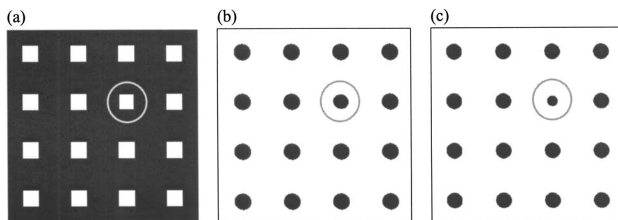

FIG. 6. Mask error enhancement factor modeling for the Berkeley MET tool. (a) Input mask, (b) resist image assuming ideal binary resist, and (c) resist image using point-spread function resist model with 20 nm blur.

ACKNOWLEDGMENTS

The authors are greatly indebted to Kevin Bradley, Stefano Cabrini, Weilun Chao, Rene Delano, Jeff Gamsby, Eric Gullikson, Bob Gunion, Gideon Jones, Ron Oort, Ron Tackaberry, and Farhad Salmassi for expert engineering, technical, and fabrication support. The authors are also grateful to Hiroto Yukawa of TOK, Seiya Masuda of Fujifilm, and Jim Thackeray and Katherine Spear of Rohm and Haas for resist support. This work was supported by SEMATECH and carried out at Lawrence Berkeley National Laboratory's Advanced Light Source, which is supported by the DOE, Office of Science, Basic Energy Sciences.

[1]Proceedings of the Fourth International EUVL Symposium Steering Committee, San Diego, CA, 7–9 November 2005, proceedings available from SEMATECH, Austin, TX.
[2]Proceedings of the 2006 International Symposium on Extreme Ultraviolet Lithography Steering Committee, Barcelona, Spain, 15–18 October 2006, proceedings available from SEMATECH, Austin, TX.
[3]P. Naulleau *et al.*, Proc. SPIE **5374**, 881 (2004).
[4]A. Brunton *et al.*, Proc. SPIE **5751**, 78 (2005).
[5]H. Oizumi, Y. Tanaka, I. Nishiyama, H. Kondo, and K. Murakami, Proc. SPIE **5751**, 102 (2005).
[6]H. Meiling *et al.*, Proc. SPIE **6151**, 615108 (2006).
[7]M. Miura, K. Murakami, K. Suzuki, Y. Kohama, Y. Ohkubo, and T. Asami, Proc. SPIE **6151**, 615105 (2006).
[8]P. Naulleau, K. Goldberg, E. Anderson, K. Dean, P. Denham, J. Cain, B. Hoef, and K. Jackson, J. Vac. Sci. Technol. B **23**, 2840 (2005).
[9]J. Cain, P. Naulleau, and C. Spanos, J. Vac. Sci. Technol. B **24**, 326 (2006).
[10]R. Soufli *et al.*, Appl. Opt. **46**, 3736 (2007).
[11]R. Hudyma, J. Taylor, D. Sweeney, L. Hale, W. Sweatt, and N. Wester, "E-D characteristics and aberration sensitivity of the Microexposure Tool (MET)," Proceedings of the Second International EUVL Workshop, 19–20 October 2000, proceedings available from SEMATECH, Austin, TX.
[12]P. Naulleau, K. Goldberg, P. Batson, J. Bokor, P. Denham, and S. Rekawa, Appl. Opt. **42**, 820 (2003).
[13]C. Anderson, P. Naulleau, P. Denham, D. Kemp, and S. Rekawa, "Dual-Domain Scanning Illuminator for the SEMATECH Berkeley Microfield Exposure Tool," these proceedings.
[14]P. Naulleau, P. Denham, and S. Rekawa, Opt. Eng. **44**, 13605 (2005).
[15]P. Naulleau, C. Anderson, K. Dean, P. Denham, K. Goldberg, B. Hoef, B. La Fontaine, and T. Wallow, Proc. SPIE **6517**, 6517OV (2007).
[16]P. Naulleau, J. Cain, and K. Goldberg, Appl. Opt. **45**, 1957 (2006).
[17]P. Naulleau, J. Cain, and K. Goldberg, J. Vac. Sci. Technol. B **23**, 2003 (2005).
[18]K. Goldberg, P. Naulleau, P. Denham, S. Rekawa, K. Jackson, E. Anderson, and J. Liddle, J. Vac. Sci. Technol. B **22**, 2956 (2004).
[19]C. Ahn, H. Kim, and K. Baik, Proc. SPIE **3334**, 752 (1998).
[20]P. Naulleau, Appl. Opt. **43**, 788 (2004).
[21]G. Gallatin, Proc. SPIE **5753**, 38 (2005).